

Polarizability of red blood cells with an anisotropic membrane

José Luis Sebastián, Sagrario Muñoz, Miguel Sancho, and Genoveva Martínez

Departamento de Física Aplicada III, Facultad de Ciencias Físicas, Universidad Complutense, 28040 Madrid, Spain

Karan V. I. S. Kaler

Schulich School of Engineering, Department of Electrical and Computer Engineering, University of Calgary, Calgary, Canada T2N 1N4

(Received 5 October 2009; revised manuscript received 2 December 2009; published 1 February 2010)

We predict the complex polarizability of a realistic model of a red blood cell (RBC), with an inhomogeneous dispersive and anisotropic membrane. In this model, the frequency-dependent complex electrical parameters of the individual cell layers are described by the Debye equation while the dielectric anisotropy of the cell membrane is taken into account by the different permittivities along directions normal and tangential to the membrane surface. The realistic shape of the RBC is described in terms of the Jacobi elliptic functions. To calculate the polarizability, we evoke the effective dipole moment method to determine the cell internal electric field distribution, employing an adaptive finite-element numerical approach. We have furthermore investigated the influence of the anisotropic membrane and dispersive electrical parameters of each individual cell layer on the total complex polarizability. Our findings suggest that the individual layer contribution depends on two factors: the volume of the layer and the associated induced electric field, which in turn is influenced by other layers of the cell. These results further show that the average polarizability spectra of the cell are significantly impacted by the anisotropy and associated dispersion of the cellular compartments.

DOI: [10.1103/PhysRevE.81.022901](https://doi.org/10.1103/PhysRevE.81.022901)

PACS number(s): 87.50.-a

I. INTRODUCTION

In previous work [1], we presented a method for calculating the polarizability tensor α of a shelled piecewise homogeneous particle of arbitrary shape when immersed in lossy media. The focus of this investigation was to study the impact of shape on the polarizability. In the present Brief Report, we determine the polarizability of a realistic anisotropic shelled red blood cell (RBC) model with both a dispersive membrane and cytoplasm. We assume that the anisotropic membrane dielectric function is different along the directions normal and tangential to the membrane surface and analyze the contributions of each anisotropic and dispersive layer to the total complex polarizability of the cell. Therefore, in this work, the term “realistic” applies both to the geometry and electrical composition of the cell. The principal thrust in calculating α in terms of electric and geometric parameters of the RBC is to provide more quantitative information of the cell morphology [2] and interaction of the cellular matter with em fields.

Although there is a general formula for determining the polarizability of a homogeneous particle of arbitrary shape [3], however similar generalization suitable for more realistic models of particles with complex geometries and several layers of different lossy dielectric media is rather difficult to implement. Thus to determine the polarizability of a RBC subjected to a periodic electric field, this requires the calculation of the internal electric field distribution, for which we resort to an adaptive finite-element (FE) numerical method. To analyze all possible relaxation phenomena, we consider the effect of an externally applied ac electric field, covering a broad frequency range extending from 10 kHz to 3 GHz.

In order to facilitate ready comprehension of this work, in Sec. II we recapitulate the expression of the polarizability, originally derived in Ref. [1] and the set of parametric equations used to generate the realistic shape of all layers of the

RBC. We furthermore introduce the Debye dispersion equations to describe the permittivity and conductivity of the different layers of the cell as well as the anisotropic conductivity of the membrane as a function of the polarization of the applied electric field. In Sec. III, we present the results obtained for the complex polarizability along the principal axes of the RBC and analyze the contribution of each compartment to its total polarizability. We conclude our Brief Report (in Sec. IV) with a discussion and summary of our findings.

II. POLARIZABILITY AND ANISOTROPIC RBC MODEL

We can calculate the polarizability of a RBC, which is immersed in a lossy surrounding medium, by considering the mechanical response of the cell to an external EF. To a first approximation, this force on the dielectric particle or cell can be calculated as that produced by the field acting on an induced dipole. In this case, an effective dipole moment of the particle has to be determined in order to properly take into account the reaction effect of the external medium and the complex character of the permittivity of both the particle and surrounding medium. By using this approach we circumvent the cumbersome process of the integration of the Maxwell stress tensor over the particle or cell surface. The authors have shown [1] that the effective polarizability tensor of a particle comprised of N layers that is immersed into a field region \vec{E}_0 established in a homogeneous isotropic and linear medium 1, characterized by a complex permittivity $\tilde{\epsilon}_1 = \epsilon_1 - i\sigma_1/\omega$ can be calculated from

$$\tilde{\alpha}_{eff}\vec{E}_0 = \frac{\text{Re}(\tilde{\epsilon}_1)}{\tilde{\epsilon}_1} \sum_{i=1}^N \int_{V_i} (\tilde{\epsilon}_i - \tilde{\epsilon}_1) \vec{E}_i dV_i, \quad (1)$$

where $\tilde{\epsilon}_i$, \vec{E}_i , and V_i are the complex permittivity, the internal electric field distribution, and the volume, respectively, of the layer i .

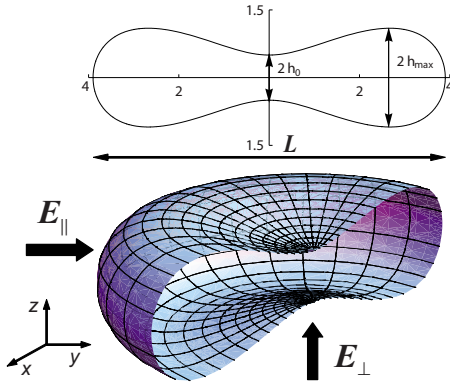


FIG. 1. (Color online) Two-dimensional (2D) and 3D geometrical models of the RCB. Cell dimensions: $L=7.8 \mu\text{m}$, $h_0=0.5 \mu\text{m}$, $h_{\text{max}}=1.09 \mu\text{m}$, $\delta_{\text{memb}}=8 \text{ nm}$, and total cell volume $V=86.13 \mu\text{m}^3$. The cell is suspended in an external medium and \vec{E}_\perp and \vec{E}_\parallel are the normal and parallel polarizations, respectively, of the external EF.

Note that the two multiplicative factors $\varepsilon_0(\tilde{\varepsilon}_i - \tilde{\varepsilon}_1)/\tilde{\varepsilon}_1$ and $\text{Re}(\tilde{\varepsilon}_1)/\varepsilon_0$ are included in the definition of $\tilde{\mathbf{p}}_{\text{eff}}$. The first one comes from the fact that the situation of a dielectric particle in the external field is analogous to that of a body immersed in a fluid under a gravitational field. Thus when calculating the net force, we must similarly subtract a buoyancy term. The second factor $\text{Re}(\tilde{\varepsilon}_1)/\varepsilon_0$ arises from considering that the equivalent charges and dipole are situated in vacuum so that the external field has to be multiplied by the relative inductive factor of vacuum and medium. Also, it is worth noting that the integration is performed only over the volume V of the particle.

Therefore, the three components of the effective polarizability tensor for an anisotropic particle with arbitrary shape can be obtained as follows: we apply the external field \vec{E}_0 , calculate numerically the field \vec{E}_i in every compartment of the cell as described in Sec. III, and perform the integrations in Eq. (1). With three orientations of the external field, with respect to the particle, we can determine the full tensor.

To model the geometry and different layers of the RBC we have used the set of parametric equations, in terms of the Jacobi elliptic functions, described in Refs. [1,4]. The schematic and three-dimensional (3D) model representations of the RBC and the numerical values [5] that we have used are shown in Fig. 1.

In this contributing work we have used a RBC structure formed by cytoplasm and a single layer membrane that is suspended in an electrolyte and exposed to an impinging external field of amplitude $E_0=1 \text{ V/m}$ of variable frequency, covering a range from 10 kHz to 3 GHz. We have furthermore focused on the contributing role played by the anisotropy and dispersion of the membrane in the electrical response of RCBs. This interest is based on two important considerations; the first one is that the membrane is a locus of electric field amplification. The amplification factor in the electric field from the external medium to the membrane is a function of the membrane permittivity, and this factor may vary anywhere from 5 to 30 [6]. The second consideration is that we have to take into account the presence of tangential

conductance along the cell membrane, which originates from the presence of excess positive ions in the diffused electric double layer induced by the negatively charged groups of glycolipids located on the cell membrane surface [7,8]. Therefore, we have considered that the permittivity and conductivity of the membrane are characterized by the dispersion equations when the field (\vec{E}_\parallel) is parallel to the x or y axis, whereas they have constant values when the external electric field (\vec{E}_\perp) is parallel to the z axis of the cell [9–11]. Since there is little evidence of anisotropies in the dielectric properties of the external medium and cytoplasm, we have assumed that they show an isotropic behavior and that the permittivity and conductivity of these regions follow the same dispersion equations, which are discussed below for both polarizations of the external field [12].

In the case of a polar liquid, with a single relaxation time constant, the frequency-dependent permittivity and conductivity can be expressed by the classical Debye equation [13]

$$\varepsilon_r = \varepsilon_{r\infty} + \frac{\Delta\varepsilon_r}{1 + \omega^2\tau^2}, \quad (2)$$

$$\sigma = \sigma_s + \frac{\Delta\varepsilon_r\varepsilon_0\omega^2\tau}{1 + \omega^2\tau^2}, \quad (3)$$

where τ is the characteristic relaxation time, σ_s is the “static” conductivity, ε_{rs} and $\varepsilon_{r\infty}$ are the values of permittivity at frequencies much smaller than $1/\tau$ (static) and much higher than $1/\tau$ (high frequency), respectively, and $\Delta\varepsilon_r = \varepsilon_{rs} - \varepsilon_{r\infty}$ is the relative dielectric decrement.

Table I shows the values of the parameters that we use in Eqs. (2) and (3) for each cellular compartment obtained from literature [14–18]. For the case of an isotropic membrane, we use the values corresponding to normal polarization.

III. ANALYSIS OF THE RBC POLARIZABILITY

To determine the internal electric field distributions within the different layers of the RBC, we have used the adaptive FE mesh software ANSOFT [19]. The cell is centered in a cube (radiation region) filled with an external medium characterized by the electrical parameters shown in Table I. We have considered two polarizations for the external field of magnitude $E_0=1 \text{ V/m}$ applied over the two opposite faces of the cube: the “normal orientation ($\alpha_\perp = \alpha_z$)” where the electric vector \vec{E}_\perp is aligned with the minor axis z of the RBC, and the “parallel orientation ($\alpha_\parallel = \alpha_y = \alpha_x$)” with the electric vector \vec{E}_\parallel is aligned with a major axis (x or y) of the cell (cf. Fig. 1). We have also implemented several technical improvements to ensure the generation of a clean mesh and to reduce error and computation time [1].

Figure 2 shows the results for the real and imaginary parts of the complex polarizability of the RBC model with an anisotropic membrane. For comparison purposes, we have also included the results for the cell model with the same structure but with an isotropic membrane (cf. note in Table I). We see in Fig. 2(a) that when the external field is applied parallel to the principal z axis both models predict the same polarizability response as expected. The value of the normal

TABLE I. Electrical and geometrical parameters of the RBC model.

Medium	ϵ_{rs}	$\epsilon_{r\infty}$	σ_s (S m ⁻¹)	τ (s)	Vol (μm^3)
Cytoplasm	50	1.8	0.53	8.8×10^{-12}	85.02
Cytoplasmic BW	7.51	6.85	2.626	4.6×10^{-10}	0.05
Membrane normal ^a	5	5	1×10^{-6}		1.01
Membrane tangential	151.3	5	1×10^{-6}	3.1×10^{-9}	
Extra-cellular BW	11.916	11.256	0.02626	4.6×10^{-10}	0.05
External medium	80	1.8	0.12	8.8×10^{-12}	

^aValues used for the isotropic case.

membrane conductivity is very small over the entire frequency range and practically imposes no attenuation on the normal component of the induced electric field. However, when the external field is applied along the principal y axis, the real and imaginary parts of the anisotropic polarizability reach significant higher values than for the isotropic case. Also, both curves are shifted toward lower frequencies, with the real part exhibiting a plateau region and the imaginary part a wide transition region between maximum positive and minimum negative values.

We may explain the observed changes in the polarizability curves by analyzing the contribution of each layer of the cell to the total polarizability. To this end, we should remark that the expression for the polarizability that we derived in Sec. II has the form of a weighted average with weights determined by the differences in permittivities between the layers and the external medium and that the induced field distribution within a particular layer is controlled by all layers of the cell.

Figure 3 shows the contributions of the membrane and cytoplasm to the right-hand side of Eq. (1) for both polarizations of the external field. When the external field is applied along the z axis, Fig. 3(a) shows that at low frequencies, the most significant contribution to the real part of the polarizability comes from the membrane, whereas at high frequencies it comes from the cytoplasm. However, the contributions to the imaginary part from the membrane and cytoplasm are very similar in the full frequency range. Figure 3(b) shows very different results when the external field is applied along the y axis. For this orientation of the field, the spectrum of

the real part of the polarizability is mainly governed by the cytoplasm. The contribution of the membrane at intermediate and high frequencies is very small due to its high conductivity value and smaller volume. It is important to note, that although the induced electric field within the cytoplasm has a low value for both polarizations [16], the cytoplasm has a much larger volume than the membrane and therefore leads to a significant contribution to the right-hand side of Eq. (1).

IV. CONCLUSIONS

The principle focus in this Brief Report has been the calculation of the complex polarizability of a realistic RBC, with an inhomogeneous dispersive and anisotropic cell structure. To calculate the polarizability, we have used the induced effective dipole moment approach, which was originally derived by the authors in a previous work for single shelled cells. This approach leads to an expression of the polarizability in terms of the induced electric field distribution, the volume, and the complex permittivities of the cell constituents and has the form of a weighted average with weights determined by the differences in permittivities between the shells and the external medium. The induced electric field within the different layers is determined by a finite-element numerical technique using adaptive meshing and some additional technical improvements.

We have used dispersion equations for the conductivity and permittivity for all layers based on previous electrical properties of the cell compartments accepted in the literature.

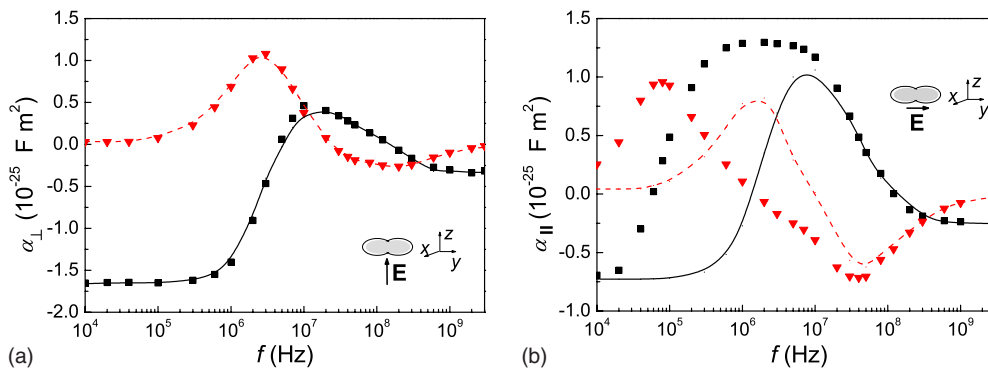


FIG. 2. (Color online) Comparison between the calculated complex polarizability components of an RBC with isotropic membrane (lines) and with anisotropic membrane (markers) as a function of frequency f , (a) α_{\perp} , and (b) α_{\parallel} . The solid line and squares mark the real part of the polarizability, while the dashed line and triangles represent the imaginary part.

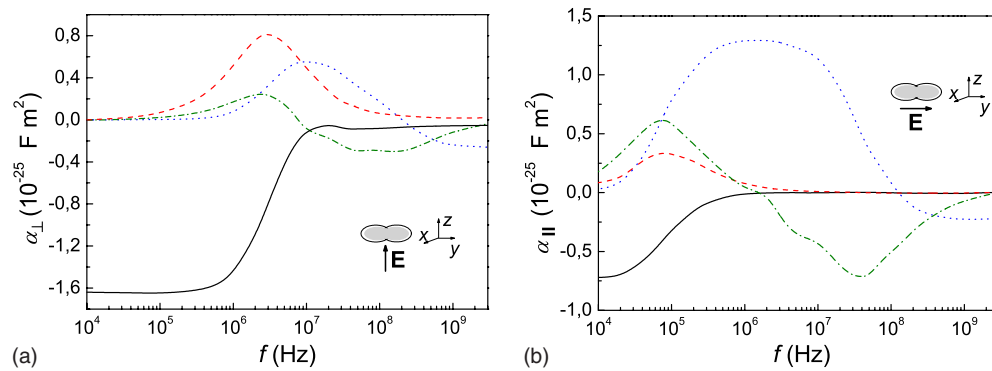


FIG. 3. (Color online) Contributions of the membrane and cytoplasm to the total complex polarizability of the RBC as a function of frequency f , (a) α_{\perp} , and (b) α_{\parallel} . The solid and dashed interpolated lines mark the real and imaginary parts, respectively, of the membrane polarizability, while dotted and dash-dotted interpolated lines represent the real and imaginary parts, respectively, of the cytoplasm polarizability.

The dielectric anisotropy in the membrane has been considered in terms of different conductivities along the minor and major axes of the cell. Depending on the orientation of the applied field, we have observed that the dielectrically anisotropic membrane leads to results for the real and imaginary parts of the polarizability that are substantially different from the values we obtained with the isotropic membrane. To get a better understanding of these differences, we analyzed the contribution of each layer to the total complex polarizability by taking advantage of the fact that integrations in the expression of the polarizability are performed over the volume of each layer. We put a strong emphasis on the fact that the induced field distribution within a particular layer is controlled by all layers of the cell. Therefore, a given layer that provides a small contribution to the total polarizability can play however a fundamental role in the field within another

layer that has a much higher contribution. This explains the characteristic curve for the complex polarizability along the major axis of the RBC.

Although we have focused our interest in RBCs, the approach used in this work can be readily applied to study electromechanical effects in different types of particles with arbitrary shape and structure. This approach will provide a good electrical characterization of the particle as long as the particle is realistically represented. The calculation time will depend on the complexity of the geometry and the inner structure of the particle.

ACKNOWLEDGMENT

This work was supported by the Comunidad de Madrid (Bioelectromagnetism Research Group 910305).

-
- [1] J. L. Sebastián, S. Muñoz, M. Sancho, and G. Álvarez, *Phys. Rev. E* **78**, 051905 (2008).
 [2] E. Gheorghiu, *Ann. N. Y. Acad. Sci.* **873**, 262 (1999).
 [3] A. G. Ramm, *Wave Scattering by Small Bodies of Arbitrary Shape* (World Scientific, Singapore, 2005).
 [4] J. L. Sebastián, S. M. San Martín, M. Sancho, J. M. Miranda, and G. A. Alvarez, *Phys. Rev. E* **72**, 031913 (2005).
 [5] H. J. Deuling and W. Helfrich, *Biophys. J.* **16**, 861 (1976).
 [6] S. Muñoz, J. L. Sebastián, M. Sancho, and J. M. Miranda, *Phys. Med. Biol.* **48**, 1649 (2003).
 [7] V. L. Sukhorukov, G. Meedt, M. Kürschner, and U. Zimmermann, *J. Electrostat.* **50**, 191 (2001).
 [8] M. Simeonova and J. Gimsa, *J. Phys.: Condens. Matter* **17**, 7817 (2005).
 [9] P. Läger, R. Benz, G. Stark, E. Bamberg, P. C. Jordan, A. Fahr, and W. Brock, *Q. Rev. Biophys.* **14**, 513 (1981).
 [10] M. Kürschner, K. Nielsen, C. Andersen, V. L. Sukhorukov, W. A. Schenk, R. Benz, and U. Zimmermann, *Biophys. J.* **74**, 3031 (1998).
 [11] H. A. Stern and S. E. Feller, *J. Chem. Phys.* **118**, 3401 (2003).
 [12] J. Gimsa, T. Müller, T. Schnelle, and G. Fuhr, *Biophys. J.* **71**, 495 (1996).
 [13] K. R. Foster and H. P. Schwan, *Crit. Rev. Biomed. Eng.* **17**, 25 (1989).
 [14] M. Simeonova and J. Gimsa, *Bioelectromagnetics (N.Y.)* **27**, 652 (2006).
 [15] L. M. Liu and S. F. Cleary, *Bioelectromagnetics (N.Y.)* **16**, 160 (1995).
 [16] B. Klösgen, C. Reichle, S. Kohlsmann, and K. Kramer, *Biophys. J.* **71**, 3251 (1996).
 [17] H. Frischleder and G. Peinel, *Chem. Phys. Lipids* **30**, 121 (1982).
 [18] M. Brecht, B. Klösgen, C. Reichle, and K. D. Kramer, *Mol. Phys.* **96**, 149 (1999).
 [19] *ANSOFT HFSS User's Manual* (Ansoft Corporation, Pittsburgh, PA, 2002).